Journal of Medicinal Chemistry

Article

Antibiotic Binding to Monozinc CphA β-Lactamase from *Aeromonas hydropila*: Quantum Mechanical/Molecular Mechanical and Density Functional Theory Studies

Dingguo Xu, Yanzi Zhou, Daiqian Xie, and Hua Guo

J. Med. Chem., **2005**, 48 (21), 6679-6689• DOI: 10.1021/jm0505112 • Publication Date (Web): 17 September 2005

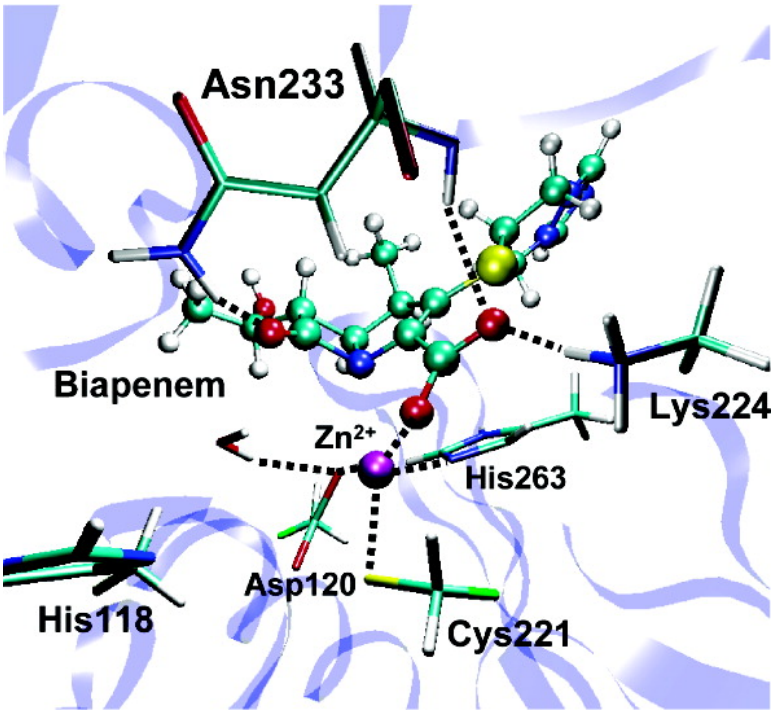

More About This Article

Additional resources and features associated with this article are available within the HTML version:

- Supporting Information
- Links to the 5 articles that cite this article, as of the time of this article download
- Access to high resolution figures
- Links to articles and content related to this article
- Copyright permission to reproduce figures and/or text from this article

Journal of Medicinal Chemistry is published by the American Chemical Society. 1155 Sixteenth Street N.W., Washington, DC 20036

Antibiotic Binding to Monozinc CphA β-Lactamase from *Aeromonas hydropila*: Quantum Mechanical/Molecular Mechanical and Density Functional Theory Studies

Dingguo Xu,[†] Yanzi Zhou,[‡] Daiqian Xie,[‡] and Hua Guo*[,†]

Department of Chemistry, University of New Mexico, Albuquerque, New Mexico 87131, and Department of Chemistry, Institute of Theoretical and Computational Chemistry, Nanjing University, Nanjing 210093, People's Republic of China

Received June 1, 2005

The active-site dynamics of apo CphA β-lactamase from *Aeromonas hydropila* and its complex with a β-lactam antibiotic molecule (biapenem) are simulated using a quantum mechanical/molecular mechanical (QM/MM) method and density functional theory (DFT). The quantum region in the QM/MM simulations, which includes the Zn(II) ion and its ligands, the antibiotic molecule, the catalytic water, and an active-site histidine residue, was treated using the self-consistent charge density functional tight binding (SCC-DFTB) model. Biapenem is docked at the active site unambiguously, based on a recent X-ray structure of an enzyme−intermediate complex. The substrate is found to form the fourth ligand of the zinc ion with its 3-carboxylate oxygen and to hydrogen bond with several active-site residues. The stability of the metal−ligand bonds and the hydrogen-bond network is confirmed by 500 ps molecular dynamics simulations of both the apo enzyme and the substrate−enzyme complex. The structure and dynamics of the substrate−enzyme complex provide valuable insights into the mode of catalysis in such enzymes that is central to the bacterial resistance to β-lactam antibiotics.

I. Introduction

β-Lactam antibiotics, such as penicillins, cephalosphorins, and carbapenems, have been widely and successfully used in treating bacterial infections. These molecules operate by forming a covalent adduct with membrane-bound bacterial transpeptidases, which are also known as penicillin-binding proteins (PBPs), involved in the biosynthesis of cell walls.[1,2] These mechanism-based inhibitors prevent the construction of the cell wall and lead eventually to cell lysis and death. In the last 20 years, however, the efficacy of these antibiotics has been overshadowed by the emergence of drug-resistant bacterial strains resulting from evolutionary responses to widespread overuse and abuse of antibiotics in clinical and agricultural settings. The problem has escalated to a crisis level, posing serious public-health and economic challenges to modern society.[3] Consequently, there is an urgent need to understand the mechanism of resistance, which may lead to novel and more effective drugs.[2,4]

The most common and effective strategy of bacterial resistance is through β-lactamases, which inactivate β-lactam antibiotics by hydrolyzing the C−N bond in the lactam ring.[1,2,4−6] The β-lactamase family can be divided into four classes on the basis of functional characteristics.[7,8] A, C, and D classes are serine β-lactamases, which employ an active-site serine residue for catalysis. Class B consists of metallo-β-lactamases that require one or two divalent zinc cofactors and use an active-site H_2O/OH^- in hydrolysis. The serine-based β-lactamases are distantly related to the PBPs, but the origin of metallo-β-lactamases is still not clear. Among the four classes, class A β-lactamases are the most prevalent in the clinical setting and have consequently been more extensively studied.[4] However, there is a growing concern about the class B β-lactamases despite their relatively small population.[9,10] Their broad substrate spectra and the absence of clinically useful inhibitors render them a potentially more dangerous threat to the relatively small arsenal of β-lactam antibiotics. An alarming trend in recent years points to a rapid spread of these metalloenzymes in pathogenic microorganisms by plasmid-mediated gene exchanges.[10,11]

Class B β-lactamases can be further divided into three subclasses.[9,12] Subclass B1 enzymes are found in *Bacillus*, *Bacteroides*, *Pseudomonas*, *Serratia*, and *Chryseobacterium*, whereas subclass B3 enzymes exist in *Stenotrophomonas*, *Legionella*, *Fluoribacter*, *Janthinobacterium*, and *Caulobacter*. Subclass B2 enzymes, however, have only been found in *Aeromonas*. These metalloenzymes have considerable sequence diversity, sharing only 25−40% sequence similarities within a subclass and 10−20% between subclasses.[12,13] Despite their low sequence homology, the key catalytic motifs are largely conserved.

The catalytic mechanism of class B β-lactamases is still not completely resolved,[13] but it is clear that at least one divalent zinc ion is needed. Structural studies have shown that all class B β-lactamases possess two potential binding sites for Zn(II) near the bottom of a broad crevasse.[14−22] The so-called Zn1 site is comprised of three His residues in the B1 and B3 subclasses, but one His is replaced by Asn in the B2 subclass. On the other hand, the Zn2 site consists of an Asp-Cys-His triad in the B1 and B2 subclasses and an Asp-His-His triad in the B3 subclass, respectively. It is known that both B1

* Corresponding author. E-mail: hguo@unm.edu. Phone: 505-277-1716. Fax: 505-277-2609.
[†] University of New Mexico.
[‡] Nanjing University.

10.1021/jm0505112 CCC: $30.25
Published on Web 09/17/2005

and B3 subclass β-lactamases are catalytically active with either one or two zinc cofactors.[21,23−28] However, only the monozinc form possesses catalytic activity for subclass B2 enzymes.[29,30] The hydrolysis of the lactam amide bond is believed to be accomplished by an active-site H_2O/OH^-, which attacks the carbonyl carbon in the lactam ring.[13] The mechanistic details of the reaction are still sketchy.

Elucidation of the catalysis cannot be achieved without a clear understanding of the substrate binding. Unfortunately, the binding of antibiotic molecules in the active site of metallo-β-lactamases is poorly understood because the high efficiency of the enzyme prevents structural determination of the Michaelis complex. Indeed, the current knowledge concerning substrate binding has largely been extrapolated from X-ray structures of apo enzymes[14−19] and of enzyme−inhibitor/intermediate complexes.[31−34] More recently, computational simulations have started to provide microscopic insight into the structure and dynamics of substrate−enzyme complexes.[35−44] For instance, simulations[36,43] have confirmed an interesting experimental finding that an active-site loop structure appears to be involved in substrate binding.[45,46] However, the modeling of substrate binding often faces difficulties stemming from the fact that many conformations are possible for the substrate to make productive interactions with the metal(s) and the active-site residues. This is particularly problematic for subclass B1 and B3 enzymes because of their broad substrate profiles. Theoretically, it is a challenge to design force fields that can accurately account for the metal−ligand interaction.[43] Hence, it is desirable to treat the substrate and the metal−ligand complex quantum mechanically, as suggested recently by a number of groups.[41,44]

An ideal approach to the study of enzymatic reactions is the use of quantum mechanical/molecular mechanical (QM/MM) models,[47−50] which partition the system into a QM region and a classical MM region. The QM region includes the reacting species and some other moieties that are expected to be significantly involved in the reaction, while the surrounding MM region provides a realistic reaction field. A force field approach is often sufficient for describing the MM atoms, as their thermal motion is largely near their equilibria. On the other hand, a quantum description of the potential for the reactive QM atoms is necessary. Obviously, the QM/MM approach represents a compromise, but numerous studies have demonstrated that it is an effective scheme to characterize enzymatic reactions.[51−54] Indeed, QM/MM studies of the metallo-β-lactamases have been reported, primarily by the Merz group[37,44,55] and the Carloni group.[56] For the QM part, the Merz group relies on a newly developed PM3 parametrization designed for zinc-containing enzymes,[57] while the Carloni group uses the Car−Parrinello method with density functional theory (DFT).

In this publication, we present theoretical studies of the substrate binding by a subclass B2 β-lactamase using an alternative QM/MM approach based on a recently proposed self-consistent charge density functional tight binding (SCC-DFTB) method.[58] The SCC-DFTB method is an approximate density functional theory based on a second-order expansion of the total DFT energy with respect to the charge density variation.[58] It represents an improvement of the original DFTB method because of a self-consistent procedure which iteratively relaxes the atomic Mulliken charges and has been shown to give quite accurate results for the geometry,[59,60] vibrational frequencies,[61,62] and reaction energies[59,60,63] for many molecular systems. In addition to its accuracy, the SCC-DFTB approach is also very efficient, with a speed comparable to that of most other semiempirical methods such as AM1 and PM3. The efficiency derives from the parametrization of the Hamiltonian as a function of internuclear distances. As a result, it has been applied to many biological systems with impressive results.[59,63−71] A particularly important advance related to this work is the recent parametrization of biological zinc, which yielded results such as geometry and ligand binding energies that are much better than those of the original PM3 method, as compared with the B3LYP/6-311+G(d,p) level of theory.[71] This advance opens the door for simulating many zinc-containing enzymes, such as carbonic anhydrase,[72] cytidine deaminase,[73,74] and metallo-β-lactamases, in this work.

Our work is motivated by recent X-ray diffraction studies of the CphA metallo-β-lactamase from *Aeromonas hydropila* and its complex with a reaction intermediate.[20] These structures are unique in several respects. First, the zinc ion was found in the apo enzyme at the Zn2 site, rather than at the Zn1 site commonly found in subclass B1/B3 β-lactamases.[14] This striking feature is corroborated by spectroscopic evidence from β-lactamases from *A. hydrophila*[30,75] and *A. veronii*.[76] More importantly, the structural work established that the zinc binding site in this enzyme is not changed upon binding of the substrate. This is an important point that has not been fully established for subclass B1 and B2 mononuclear enzymes, which has led to speculations on the true location of the catalytic zinc ion under physiological conditions.[28,77] Second, it was the first report of any metallo-β-lactamase complexed with an antibiotic molecule. The structure of the enzyme−intermediate complex, thus, provides a rare opportunity and an excellent starting point for theoretical studies of the binding of antibiotics to metallo-β-lactamases.

II. Computational Methods

A. Docking Model. The general binding pattern of antibiotic molecules in the active site of metallo-β-lactamases has not been fully established because of the absence of structural information on the Michaelis complex. In addition, the mode of substrate binding may be diverse given the differences in zinc stoichiometry and the active-site environment within the metallo-β-lactamase family. For the CphA system, fortunately, the recent crystallographic structure of its complex with a reaction intermediate of biapenem hydrolysis provides valuable information on the interaction of the substrate with the active site of the enzyme.[20] In particular, the zinc ion was found to be coordinated by Asp120, Cys221, and His263, in which the former two are deprotonated and the latter uses $N_{\epsilon 2}$ in coordination. In the apo form, the fourth ligand of the zinc ion is a carbonate ion (CO_3^{2-}). In the enzyme−intermediate complex, however, the zinc ion is ligated by the 3-carboxylate of the substrate and the lactam nitrogen after cleavage of the C−N bond. In addition, the non-metal-binding oxygen of the carboxylate is hydrogen bonded with the side chain of Lys224 and the backbone NH group of Asn233. These structural features narrow the configuration space sufficiently to

Scheme 1. Structure of Biapenem and Atomic Definition

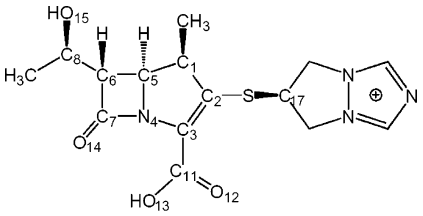

allow unambiguous docking of the substrate in the active site of the enzyme.

The structure of biapenem (Scheme 1) has been reported experimentally by small-molecule X-ray crystallography.[78] Its optimized geometry has also been determined by us at the B3LYP/6-31+G(d) and SCC-DFTB levels of theory. The agreement among the two theoretical models and with the experimental geometry is quite satisfactory.

The docking model was constructed by modifying the enzyme−intermediate complex (Protein Data Bank code 1X8I).[20] After removing the intermediate, the optimized biapenem structure was docked in the active site by placing the lactam nitrogen (N_4) and a 3-carboxylate oxygen (C_{13}) at their corresponding positions in the X-ray structure of the enzyme−intermediate complex. The substrate fits the active site reasonably well, as no obvious overlap of atoms was found. The substrate was then allowed to relax with all other protein atoms and crystallographic waters fixed. The resulting complex was then solvated and optimized according to the QM/MM protocol detailed below. The energy minimized structure is quite robust and appears to be insensitive to small variations in the initial geometry. The apo enzyme required no such manipulations, and the starting geometry was directly taken from the experimental structure (Protein Data Bank code 1X8G).

An important problem concerning the active-site structure and catalysis is the location of the catalytic water. In our docking model, this water molecule is located between His118 and Asp120, as in the X-ray structure of the enzyme−intermediate complex.[20] The presence of this water molecule in the enzyme−substrate complex will not be known for sure until its structure is determined. However, our docking model is supported by the existence of a water molecule in the same location of the apo enzyme as observed in its X-ray structure.[20]

B. QM/MM Model and Simulation Protocol. All simulations were carried out using the CHARMM suite of molecular simulation codes.[79] We chose to simulate the substrate binding using a QM/MM strategy not only because it avoids the development of empirical force field parameters but also because it sets the stage for future QM/MM studies of the catalysis mechanism. In an ideal QM/MM model, the QM part should be treated using ab initio or DFT methods. However, such a treatment is not yet computationally feasible for the large systems discussed here. In our approach, the SCC-DFTB method[58,59] was employed for the QM region, and the CHARMM all atom force field,[80] for the MM regions. The CHARMM van der Waals parameters were used for the QM atoms. The QM region of the substrate−enzyme complex contains the biapenem molecule, the zinc ion and its protein ligands, namely the side chains of Asp120, Cys221, and His263, the catalytic water, and the imidazole side chain of His118. A total of 82 atoms were included in the QM region. In the apo enzyme, the substrate was replaced by a carbonate ion and both the catalytic water and His118 were excluded from the QM region. Link atoms were introduced at the boundary,[47,49] which interact electrostatically with all MM atoms except the link hosts. In particular, the link atoms are connected to C_β atoms with C_α atoms as their link hosts. No van der Waals interaction was needed for the link atoms. The QM−MM electrostatic interactions were not truncated, while the MM−MM electrostatic interactions and all van der Waals interactions were truncated at 12 Å.

The enzyme−substrate complex obtained from the docking model was first solvated in a 25 Å radius pre-equilibrated TIP3P water[81] sphere centered at the zinc ion. Solvent water molecules found within 2.8 Å of a non-hydrogen atom or crystallographic water were deleted. The solvent sphere was allowed to relax for 30 ps with the protein atoms and crystallographic waters fixed. This process was repeated several times with randomly rotated water spheres to avoid solvent cavities. Stochastic boundary conditions[82] were imposed on the solvated system, which was divided into three near-spherical layers. The innermost reaction zone (r < 22 Å) is governed by Newtonian dynamics on the potential generated by the combined QM/MM scheme. The atoms belonging to residues in the reservoir zone (r > 25 Å) were deleted. Between these zones, the atoms in the buffer zone (22 < r < 25 Å) were subject to harmonic constraints and solvent boundary potentials, such that the system remains close to the experimental structure. During the simulation, atoms in the buffer zone are subject to Langevin dynamics (LD) with friction and random forces stemming from the bulk solvent molecules that are not explicitly included in the simulation. In a typical simulation, 3372 protein atoms and 1232 water molecules are included in the system.

The energy of the system was first minimized using the steepest descent method to remove bad contacts, and the structure was further optimized using the adapted basis Newton−Ralphson method. In molecular dynamics (MD) simulations, the system was slowly brought to room temperature and data collection followed 100 ps equilibration at 300 K. In MD calculations, the SHAKE algorithm[83] was used to maintain the covalent bonding involving H atoms. The time step of the MD simulations was 1 fs.

C. DFT Calculations. To provide an independent check of the SCC-DFTB method, we have also carried out DFT calculations of biapenem and truncated active-site models. The Becke3−Lee−Yang−Parr (B3LYP) exchange-correlation functional[84,85] and the standard 6-31+G(d) basis set were used. The minimal energy geometry was found by geometry optimization. All DFT calculations were performed using Gaussian 03.[86]

III. Results

A. Structure of Biapenem. Carbapenems, such as imipenem, meropenem, and biapenem, are broad-spectrum β-lactam antibiotics that are most effective in treating Gram-negative bacterial infections. Although resistance to carbapenems by clinically relevant pathogenic microorganisms is still low, they are particularly susceptible to hydrolysis by subclass B2 β-lactamases such as CphA, which are also known as carbapenemases.[10,11] To test the accuracy of the SCC-DFTB method, we have optimized the geometry of biapenem at the B3LYP/6-31+G(d) level with an experimental starting geometry.[78] Since the 3-carboxylate is coordinated in the enzyme with the metal ion, we chose to work with the protonated form of biapenem.

The optimized DFT geometry of biapenem is shown in Figure 1, with several key bond lengths and bond angles. The corresponding SCC-DFTB values and experimental data are given in parentheses and in square brackets, respectively. As shown in the figure, the agreement between the SCC-DFTB and DFT results is very good. The difference in bond lengths and bond angles in the free substrate is typically on the order of a few hundredths of angstrom and a few degrees, respectively. The agreement with experimental data is also reasonable. Such good agreements are in keeping with earlier observations by other authors on the accuracy of the SCC-DFTB method[59,60] and provide supporting evidence for a SCC-DFTB/MM treatment of the active site of the Michaelis complex.

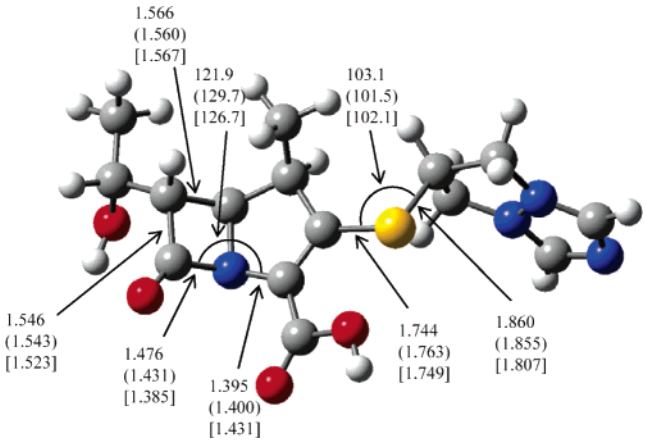

Figure 1. Comparison of biapenem geometric parameters obtained from B3LYP/6-31+G(d), SCC-DFTB (in parentheses), and experimental (in square brackets) methods. The bond lengths are given in angstroms, while the bond angles are in degrees.

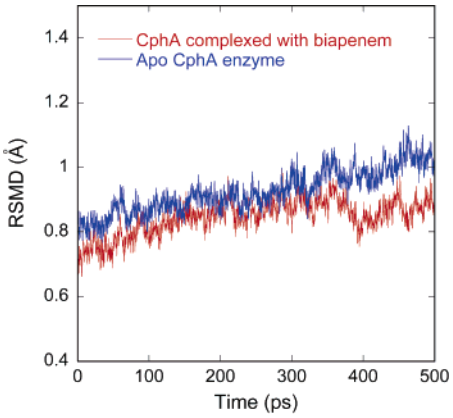

Figure 2. RMSD for the backbone atoms of the apo enzyme (blue) and the substrate−enzyme complex (red).

B. Active-Site Dynamics of the Apo Enzyme. As shown in Figure 2, the active-site structure of the apo enzyme is quite stable, as evidenced by the relatively small (<1.1 Å) root-mean-square deviation (RSMD) of the backbone atoms. The zinc ion is coordinated by four ligands, namely, the carbonate ion and the side chains of Asp120, Cys221, and His263. A typical snapshot of the metal−ligand complex is shown in Figure 3, with the relevant bond lengths and bond angles listed in Table 1. Judging from the fluctuation of these geometric parameters, the metal−ligand bonds are quite rigid and stable. This is consistent with the tight binding of the zinc ion in the Zn2 site. The comparison with experimental values lends further support to the accuracy of the SCC-DFTB model.

In addition to metal binding, the carbonate ion is also hydrogen bonded with an active-site residue (Lys224), as clearly seen in Figure 3. The hydrogen bond to the side chain of Lys224 is quite strong, as evidenced by the short O···H−N distance (1.63 ± 0.13 Å). As discussed below, a similar hydrogen bond plays a key role in the binding of biapenem to CphA. The carbonate oxygen that is bound to neither metal nor Lys224 is solvated by several waters, as shown in Figure 3. In addition, the metal-binding oxygen is also hydrogen bonded with a water molecule. Interestingly, thermal-induced cartwheel and helicopter rotations of the carbonate ion were observed to occur during the 500 ps simulation, as shown by the O−Zn distances in Figure 4. The rotation takes place within a very short time span, and the new configuration preserves the hydrogen- and metal-bonding pattern.

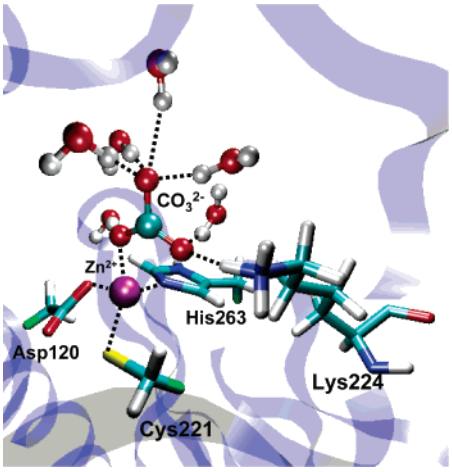

Figure 3. Snapshot of the active site of the apo CphA enzyme. Metal−ligand bonds and hydrogen bonds are indicated by dashed lines. The link atoms are shown in green.

C. Binding Dynamics of Biapenem to CphA. The CphA−biapenem complex was found to be slightly more stable than the apo enzyme, as evidenced by the small RSMD shown in Figure 2. A snapshot of the active site is displayed in Figure 5. An illustration of important metal-binding and hydrogen-bond interactions is given in Scheme 2. As in the apo enzyme, the zinc ion is tetracoordinated with the carboxylate at the substrate C_3 position as the fourth ligand, displacing the carbonate ion in the apo enzyme. The metal−ligand bonds are very similar to those in the apo enzyme, with a similar level of fluctuation, as shown in Table 1. In comparison with the X-ray structure of the enzyme−intermediate complex, the bond length between the zinc and the carboxylate oxygen (O_{13}) of the substrate is shortened from 2.39 to 2.12 ± 0.07 Å. At the same time, the distance between the zinc and the lactam nitrogen (N_4) is elongated from 2.22 Å in the X-ray structure to 3.38 ± 0.58 Å in our simulation. This is reasonable since the anionic nitrogen in the intermediate formed by cleaving the amide C−N bond has presumably a much stronger interaction with the metal cation. In the enzyme−substrate complex, on the other hand, the nitrogen is much less negatively charged because it has three covalent bonds with nearby carbon atoms.

In addition to the metal−ligand bond, the metal-binding oxygen (O_{13}) of the 3-carboxylate is also engaged in hydrogen bonding to the imidazole $HN_{\epsilon 2}$ of His196 (r(O···H−N) = 2.16 ± 0.40 Å). This His residue was observed to hydrogen bond with another oxygen (O_{15}) in the enzyme−intermediate complex.[20] On the other hand, the non-metal-binding oxygen (O_{12}) of 3-carboxylate has a strong hydrogen bond with the side chain of Lys224 (r(O···H−N) = 1.71 ± 0.12 Å), in a similar fashion as observed in the apo enzyme, and is further enhanced by another hydrogen bond to the backbone NH group of Asn233 (r(O···H−N) = 2.25 ± 0.49 Å). These interactions are probably the strongest anchoring forces for the substrate, which should be most likely retained throughout the catalysis. Indeed, the two

Table 1. Comparison of Key Geometric Parameters for the Apo CphA Enzyme and the CphA−Biapenem Complex Obtained from the SCC-DFTB/CHARMM and DFT (B3LYP/6-31+G(d)) Calculations with the Available Experimental Data

	apo CphA enzyme			CphA−biapenem complex		
distance (Å) and angle (deg)	QM/MM MD	DFT	exp	QM/MM MD	DFT	exp[a]
$N_4\cdots Zn^{2+}$				3.38 ± 0.58	3.71	2.22
$O_1/O_{13}\cdots Zn^{2+}$	2.15 ± 0.08	2.08	2.10	2.12 ± 0.07	2.03	2.39
$Zn^{2+}\cdots N_{\epsilon 2}$(His263)	2.04 ± 0.06	2.15	2.05	2.04 ± 0.07	2.07	2.13
$Zn^{2+}\cdots O_{\delta 2}$(Asp120)	2.14 ± 0.07	1.98	1.96	2.14 ± 0.07	1.98	2.03
$Zn^{2+}\cdots$ S(Cys221)	2.31 ± 0.06	2.29	2.19	2.34 ± 0.08	2.34	2.27
$O_w\cdots C_7$				3.54 ± 0.58	3.21	
$O_3/O_{12}\cdots H_{\zeta 2}$(Lys224)	1.63 ± 0.13	1.03[b]		1.71 ± 0.12	1.90	
$O_{14}\cdots H_{\delta 22}$(Asn233)				2.05 ± 0.26		
$O_{12}\cdots$H−N(Asn233)				2.25 ± 0.49		
$O_{13}\cdots H_{\epsilon 2}$(His196)				2.16 ± 0.40		
$C_7-N_4-C_3$				124.4 ± 6.4	127.7	
C_2-S-C_{17}				106.9 ± 3.5	101.7	105.4
$O_1/O_{13}\cdots Zn^{2+}\cdots O_{\delta 2}$(Asp120)	102.6 ± 8.6	101.0	102.1	124.2 ± 11.6	117.3	161.8
$O_1/O_{13}\cdots Zn^{2+}\cdots S^-$(Cys221)	112.0 ± 8.0	123.2	120.4	118.3 ± 9.7	102.4	96.3
$O_1/O_{13}\cdots Zn^{2+}\cdots N_{\epsilon 2}$(His263)	100.1 ± 12.9	93.2	101.0	95.5 ± 5.0	98.4	81.6

[a] Data from the enzyme−intermediate complex. [b] Resulting from proton transfer from the Lys side chain to the carbonate ion (see text).

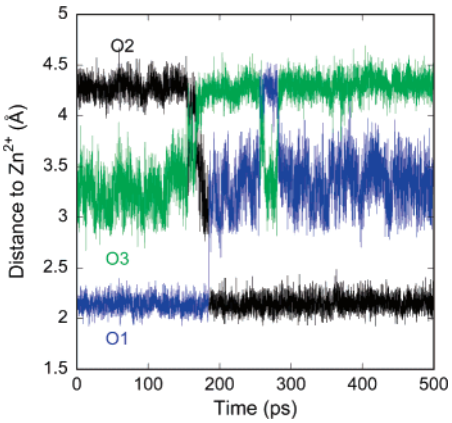

Figure 4. Distances of three carbonate oxygens from the zinc ion in the apo enzyme active site.

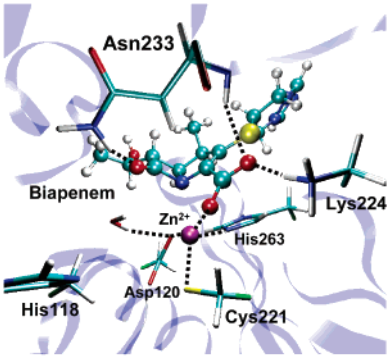

Figure 5. Snapshot of the active site of the CphA−biapenem complex. Metal−ligand bonds and hydrogen bonds are indicated by dashed lines. The link atoms are shown in green. The His196 residue is not shown in the figure to avoid congestion.

hydrogen bonds can be inferred from the X-ray structure of the enzyme−intermediate complex with O···N distances of 2.91 and 3.05 Å, respectively.

The hydrogen bond between O_{12} and the backbone NH group of Asn233 is made possible by a large conformational change of the Asn233 residue upon substrate binding. As shown in Figure 6, in which the crystal structures of the apo enzyme and the CphA−biapenem complex are compared, Asn233 moves closer to the metal center in the substrate−enzyme complex with its ψ angle rotated about 140°.[20] The conformational change

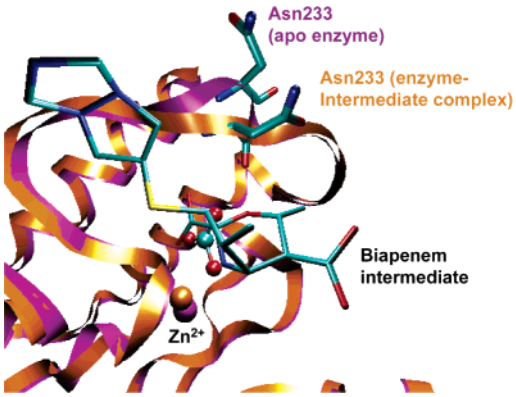

Figure 6. Overlay of the X-ray structures of the apo CphA enzyme (purple) and its complex with the biapenem intermediate (gold) clearly showing the conformational change of the Asn233 residue upon substrate binding. The biapenem substrate is displayed in tubes, while the carbonate ion is in balls-and-sticks.

Scheme 2. Important Bonding Interactions at the Active Site of the CphA−Biapenem Complex

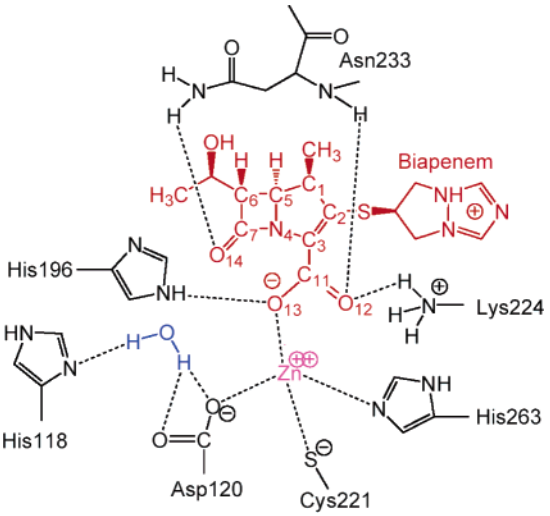

reorients the Asn side chain toward the interior of the active site and clamps the substrate. In our simulations, the average ψ angle is −36.7 ± 18.0° and 111.4 ± 10.7° for the apo and complexed forms, respectively, which can be compared to the experimental values of −18° and

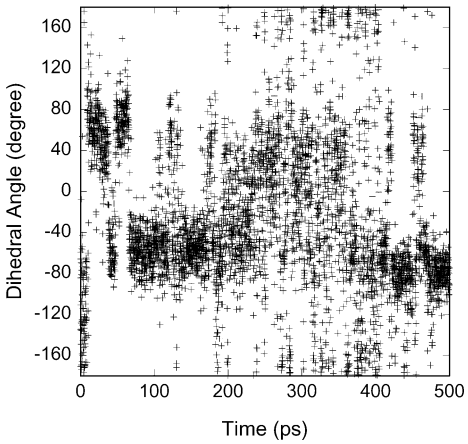

Figure 7. The H−O_{15}−C_8−C_6 dihedral angle of the hydroxyethyl group indicating facile rotational mobility.

120°. Note that the fluctuation is larger in the unbound enzyme.[20]

Augmenting the strong substrate−enzyme interactions through the 3-carboxylate group of biapenem, there are several other hydrogen bonds that also contribute to the binding. Most notable is the hydrogen bond between the lactam carbonyl oxygen (O_{14}) and the side chain NH_2 group of Asn233, as shown in Figure 5. The average hydrogen-bond distance between the oxygen and the hydrogen of the Asn NH_2 group is 2.05 ± 0.26 Å. This interaction was not noted in the X-ray structure, presumably because the intermediate observed in the X-ray study has already been hydrolyzed and the resulting carboxylate moiety has rotated to a different position.[20] This hydrogen bond is likely to serve as an "oxyanion hole" for the nucleophilic attack of the catalytic water, during which negative charge builds up at the oxygen. These hydrogen-bond interactions may be responsible for the increased stability of the enzyme−substrate complex, as implicated by the smaller RMSD in Figure 2.

Consistent with the X-ray structure, the bicyclotriazoliumthio group of the substrate is positioned between the side chains of Val67 and Lys226, pointing toward the solvent and experiencing much larger fluctuation. Apparently, its contribution to substrate binding is minimal. Indeed, other carbapenem molecules such as imipenem and meropenem have different moieties connected with the sulfur while preserving the bicyclic carbapenem rings.

Surprisingly, the hydroxyethyl group at C_6 was observed to interact weakly with the active site of the enzyme. The H−O_{15}−C_8−C_6 dihedral angle plotted in Figure 7 indicates substantial rotational flexibility. No hydrogen bond with the −OH moiety of Thr119, as suggested by Garau et al.,[20] was found. Since all carbapenem antibiotics share this moiety, its flexibility in the active site of the carbapenemase may be important for the internal rearrangement of the substrate, which is required for forming the obligatory intermediate observed in the X-ray structure.

As shown in the X-ray structure of the enzyme−intermediate, there is an active-site water near the lactam ring, which is likely the putative nucleophile that hydrolyzes the lactam amide bond. In that structure, this water is hydrogen bonded to the imidazole ring of

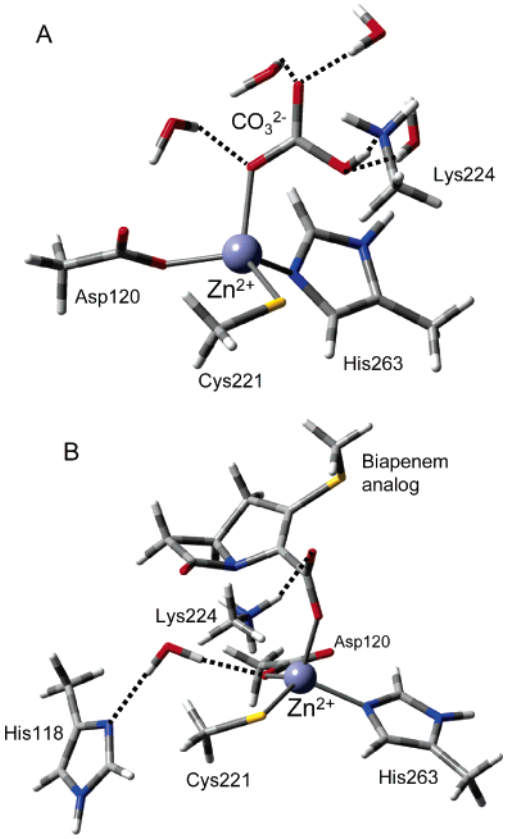

Figure 8. Geometries of the active sites of the apo CphA enzyme (A) and the CphA−biapenem complex (B) optimized at the B3LYP/6-31+G(d) level of theory. The metal−ligand and hydrogen bonds are indicated by dashed lines.

His118. In our simulation, however, this water appears to form transient hydrogen bonds primarily with a carboxylate oxygen of the metal-binding Asp120 residue, as shown in Figure 5. The imidazole of His118, which is included in the QM region, fails to make a lasting hydrogen bond to the water during the entire simulation. Furthermore, it is observed to rotate for about 180° near 190 ps, which makes the hydrogen-bond interaction even more difficult. Throughout the simulation, the motion of the catalytic water is mostly restricted in a pocket formed by His118, Asp120, and the substrate. Under no circumstances was it observed to bind with the metal. This observation disfavors the possibility that a metal-bound water serves as the nucleophile. In addition, it is well aligned with the carbonyl carbon of the substrate, evidenced by the O_w−C_7 distance of 3.54 ± 0.58 Å. It, thus, appears that the substrate-binding configuration aligns the reactants for the hydrolysis reaction in a near-attack configuration.[87]

D. DFT Models of the CphA−Biapenem Active-Site. To ensure an accurate characterization of the metal binding by the SCC-DFTB method, we have obtained minimal-energy geometries for truncated active-site models. The active-site model for the apo enzyme includes the zinc ion, the carbonate ion, an acetic acid, a methyl thiolate, a methyl imidazole to mimic the Asp120, Cys221, and His263 ligands, a methylammonium ($CH_3NH_3^+$) to mimic Lys224, and four water molecules. The optimized structure is shown in Figure 8A. Table 1 lists several key bond lengths and angles, which are in reasonable agreement with the

Table 2. ESP Charges of the Zinc Ion and Its Four Ligands in the Apo Enzyme and in the Enzyme−Substrate Complex

atom	apo enzyme	enzyme−substrate complex
Zn	0.914	0.899
$O_{\delta 2}$(Asp120)	−0.790	−0.755
S(Cys221)	−0.607	−0.625
$N_{\epsilon 2}$(His263)	−0.222	−0.222
O_1/O_{13}	−0.536	−0.546

SCC-DFTB/MM results. As shown in the figure, the carbonate ion forms a metal−ligand bond with Zn(II) and is well solvated, as seen in the QM/MM simulations. In addition, the carbonate ion is protonated by the methylamine, which also results in a hydrogen bond. We emphasize that the presence of the Lys residue is very important, as its absence leads to a bidentate binding of CO_3^{2-} to the metal and to the expulsion of the Asp120 to maintain the tetracoordination of Zn^{2+}.

The optimized structure of the active-site model for the CphA−biapenem complex is shown in Figure 8B. In this model, the carbonate ion in the apo enzyme model is replaced by a biapenem analogue and the solvent waters are substituted by a crystal water and an analogue of His118. The changes seem to have a small effect on the metal−ligand bonds, as shown in Table 1. The hydrogen bond between the Lys224 side chain and the 3-carboxylate oxygen is maintained with no proton transfer. The crystal water is hydrogen bonded to both the side chain of His118 and the side chain of Asp120. The water oxygen is only 3.21 Å away from the lactam carbonyl carbon in a near-attack configuration, similar to the case of the MD simulation in which the corresponding distance is 3.54 ± 0.58 Å.

The nature of the zinc−ligand bonds is probably best described as a mixture of covalent and electrostatic interactions. Although we did not analyze the molecular orbitals in detail, it is apparent that significant charge transfer takes place in these bonds. Table 2 lists the atomic charges of the zinc ion and its ligands in both the apo enzyme and the enzyme−substrate complex, obtained from the electrostatic potential (ESP) approach.[88,89] In particular, the charge on the zinc ion is significantly smaller than that in its free form. The covalent bond characteristics are also manifested in the well-defined tetrahedral geometry of the coordination sphere.

IV. Discussion

A. Determinants in Substrate Binding. It is well established that subclass B2 metallo-β-lactamases such as CphA strongly prefer carbapenems as substrates. This is likely due to the steric and electrostatic environment of the active site of the enzyme. Our enzyme−substrate model based on experimental structures has clearly identified the following major determinants in substrate binding in subclass B2 β-lactamases: (i) The carbapenem substrate forms a strong metal−ligand bond with the zinc ion using its 3-carboxylate oxygen. (ii) The Asn233 residue clamps down on the substrate, forming a hydrogen bond to the non-metal-binding oxygen of the 3-carboxylate of the substrate with its backbone NH group and another to the carbonyl oxygen of the substrate lactam ring with its side chain NH_2 group. (iii) These interactions are augmented by hydrogen bonds between the metal-binding oxygen of the 3-carboxylate and the His196 side chain and between the non-metal-binding oxygen of the 3-carboxylate and the backbone NH group of Asn233. (iv) The 6-hydroxyethyl group is flexible with no strong interaction with the active site. (v) The substrate −SR group is not involved in binding with the enzyme but is well solvated by the solvent waters. These binding determinants fit nicely with the bicyclic motif of carbapenem compounds.

Such a pattern is very different from the proposed binding configurations in subclass B1 and B3 β-lactamases. For those enzymes, consensus has not yet been established on the most favorable mode of substrate binding. Some believe that the antibiotic molecule is not directly metal binding;[35,37,39,41,56] others favor a carbonyl oxygen coordination with the zinc in the Zn1 site.[41,42,44,90] In a recent QM/MM docking study of benzylpenicillin to BcII,[41] for example, as many as six binding configurations were proposed. The binding pattern emerging from this work might shed some light on other metallo-β-lactamases, particularly those with two zinc cofactors.

The binding pattern suggested by the X-ray structure and by our simulations is verifiable by site-directed mutagenesis studies. For example, the N233D mutation would preserve the backbone NH group for binding the 3-carboxylate of the substrate but would not be viable to serve as the oxyanion hole for the lactam carbonyl. On the other hand, the replacement of Lys224 is expected to substantially impair the binding of a carbapenem compound. The mutation of His118 may also impact the catalysis in a significant way. These mutations have not been made experimentally.

B. Implications for Catalysis. The catalytic mechanism for subclass B1 β-lactamases is best illustrated by the hydrolysis of nitrocefin by the dinuclear CcrA from *B. fragilis*.[24,91−94] The bridging hydroxide between the two zinc ions has been suggested as the putative nucleophile.[15,16] The nucleophilic attack at the carbonyl carbon in the substrate lactam ring is shown to produce an accumulating intermediate that features an anionic nitrogen, presumably binding to Zn2. Further protonation of the nitrogen leaving group, which produces the hydrolyzed product, is rate-limiting. It is interesting to note that although a tetrahedral intermediate is known to exist in the hydrolysis of β-lactam compounds,[5] the metal ion at the Zn2 position could serve as a superacid to stabilize the anionic nitrogen leaving group sufficiently so that the tetrahedral intermediate is rendered unstable.[95] This mechanism is supported by some DFT calculations,[44,96] which found an intermediate with an anionic nitrogen binding with the zinc ion after the cleavage of the lactam C−N bond. Other subclass B1 or B3 dinuclear enzymes seem to share some important features. For example, a metal-binding reaction intermediate has also been identified for hydrolysis reactions catalyzed by the L1 metallo-β-lactamase from *S. maltophilia* (subclass B3),[97−99] which has a similar active-site structure to that of *B. fragilis*.[19]

Interestingly, the loss of one zinc ion in CcrA does not completely impair the catalytic activity of the enzyme.[24] The zinc binding site is believed to be at Zn1, based on structural studies of the less efficient mononuclear enzyme from *B. cereus*,[14,21] which also belong to subclass B1. As in the reaction catalyzed by dinuclear

enzymes, the mononuclear β-lactamase II from *B. cereus* (BcII) also produces intermediates, but in branched reaction pathways.[23] The putative nucleophile in these mononuclear enzymes such as BcII is also believed to be a zinc-bound hydroxide, but kinetic studies implicated a conserved active-site Asp residue, which has a pK_a of ~5.6 and serves as a general base to activate the OH^- nucleophile.[27,100,101] The catalytic role played by the Asp residue is supported by mutagenesis experiments[102] and recent theoretical studies.[44,55,56,96,103,104] Interestingly, the existence of a catalytic Asp residue has also been suggested by the X-ray structure[19] and a recent mutagenesis study[105] of the L1 enzyme from *S. maltophilia*, which is a dinuclear metallo-β-lactamase with the Asp residue as a metal ligand.

Unlike subclass B1 and B3 enzymes that hydrolyze a broad range of β-lactam antibiotics, the subclass B2 enzymes have a quite narrow substrate profile, containing primarily carbapenems.[10,106] More interestingly, the latter is only active in the monozinc form.[29,30] Such differences may imply diversity in the mode of catalysis among these subclasses. A significant difference from subclass B1 and B3 β-lactamases revealed by the recent X-ray[20] and spectroscopic studies[30,75,76] is the occupation of the Zn2 site. Perhaps more importantly, the active site does not contain a zinc-bound water or hydroxide. The only water molecule that is near the lactam ring is one that may hydrogen bond with the His118 and the metal-binding Asp120 residue. Given the different catalytic profile of subclass B2 β-lactamases, however, this is not entirely surprising.

It is well established that water is not a very good nucleophile and requires a general base to activate it. In CphA, such a general base may be supplied by the imidazole group of His118, as suggested by Garau et al.[20] General base catalysis by His (pK_a = 6.0) has been found in many enzymatic systems.[107] However, our simulations indicate that the hydrogen-bond interaction between the imidazole of His118 and the catalytic water is not strong. On the other hand, the active-site structures in Figures 5 and 8B suggest another possible candidate for the general base, namely, the metal-binding Asp120. The latter possibility is intriguing because a similar Asp residue has been identified in catalysis by subclass B1 and B3 β-lactamases, as mentioned above. The pK_a of Asp120 is around 4.0, and therefore, it is not a good general base in a conventional sense. Metal binding is believed to further decrease its pK_a. However, its ability to shuttle protons has been noted in many metalloenzymes, such as arginase.[108,109] We believe that the electrostatic environment at the active site of such enzymes is sufficiently strong and irregular that the proton affinity of the Asp side chain is significantly altered. This is, of course, a point that requires further theoretical study.

The catalytic role of the Asp residue is supported by mutagenic experiments[102] and theoretical studies.[44,55,56,96,103,104] Furthermore, the existence of a catalytic Asp residue has also been suggested by the X-ray structure[19] and a recent mutagenesis study[105] of the L1 enzyme from *S. maltophilia*, which is a binuclear metallo-β-lactamase with the Asp residue as a metal ligand. Hence, we believe that both reaction pathways should be included in future studies of catalytic mechanisms of these enzymes.

We can further speculate that, upon the nucleophilic addition of the OH^- group on to the carbonyl carbon of the lactam ring, the amide C−N bond will likely cleave without protonation. This is because the existence of a zinc ion can serve as a superacid to stabilize the anionic nitrogen leaving group. This speculation is supported by the X-ray structure of the enzyme−intermediate complex, which shows a nitrogen 2.22 Å away from the metal.[20] If that is indeed the case, the mechanism is then similar to that for CcrA from *B. fragilis*,[24,91−94] where an anionic nitrogen intermediate was detected spectroscopically. However, it should be realized that there might be significant rearrangement of the intermediate to accommodate the obligatory structure observed in the X-ray structure. The reaction will eventually yield the product by protonation of the metal-binding nitrogen, which is expected to weaken the metal bond to facilitate the final expulsion from the enzyme active site. Such mechanistic studies are underway in our laboratory.

V. Conclusions

Progress in simulating biosystems has advanced to an unprecedented level so that it is hard to find any experimentally interesting enzymatic systems that are not also under assault from the theoretical front.[53,54,110−112] Theoretical simulations complement experimentation by providing important microscopic details of the process and yielding quantities that are hard to measure accurately. It is important to realize that theory has not reached the level of sophistication necessary to independently predict outcomes of biological events. Rather, calculations most likely have to rely on knowledge acquired by experimental investigations. For enzyme catalysis, it is vital to build theoretical models based on experimentally obtained structural and kinetic information.

In this work, we report a quantum mechanical/molecular mechanical study of the active-site dynamics of both an apo subclass B2 metallo-β-lactamase and its complex with a potent β-lactam antibiotic molecule, biapenem. An important characteristic of our model is that it is based on the first and only existing structure of a complex of a metallo-β-lactamase with an antibiotic molecule. As a result, the model is much more free of ambiguity than previous ones. Our simulations reveal that the substrate is engaged in direct metal binding through its 3-carboxylate oxygen. It is further anchored by several hydrogen bonds between the substrate and active-site residues, particularly those made possible by the conformational change of Asn233.

An active-site water is found to reside in a pocket near the lactam carbonyl carbon of the substrate. It is found to hydrogen bond primarily with the carboxylate side chain of the metal-binding Asp120. We propose that the Asp120 residue, like His118, may serve as general base to activate the catalytic water. We further speculate that the nucleophilic attack of the lactam carbonyl carbon by the water will lead to a cleaved C−N bond and an anionic nitrogen leaving group. The latter will form a strong metal−ligand bond with the zinc ion and will eventually be protonated and leave the active site as

the product. This mechanism is consistent with the observed enzyme−intermediate structure and with a previously proposed mechanism for a binuclear β-lactamase. The QM/MM framework used in this work can be extended to study the catalytic mechanism and yield microscopic rate constants that can be compared directly with experimental data. Work in this direction is already underway in our laboratories.

A molecular-level understanding of the binding and catalysis of metallo-β-lactamases is essential in unraveling the origin of bacterial resistance and in designing novel and effective inhibitors. Progress in this important research area is likely to benefit from the interaction between experimental and theoretical investigations.

Acknowledgment. We would like to express our gratitude to Prof. Q. Cui for his valuable help with the SCC-DFTB/CHARMM simulations. This work was funded by the U.S. National Science Foundation (MCB-0313743) and by the Natural Science Foundation of China (No. 30370337). Parts of the calculations were carried out at the National Center for Supercomputing Applications.

Supporting Information Available: Optimized DFT coordinates of the active-site models. This material is available free of charge via the Internet at http://pubs.acs.org.

References

(1) Knowles, J. R. Penicillin resistance: The chemistry of β-lactamase inhibition. *Acc. Chem. Res.* **1985**, *18*, 97−104.
(2) Walsh, C. Molecular mechanisms that confer antibacterial drug resistance. *Nature* **2000**, *406*, 775−781.
(3) Neu, H. C. The crisis in antibiotic resistance. *Science* **1992**, *257*, 1064−1073.
(4) Fisher, J. F.; Meroueh, S. O.; Mobashery, S. Bacterial resistance to β-lactam antibiotics: Compelling opportunism, compelling opportunity. *Chem. Rev.* **2005**, *105*, 395−424.
(5) Page, M. I. *The Chemistry of β-Lactams*; Blackie Academic and Professional: London, 1992.
(6) Frere, J.-M. β-Lactamase and bacterial-resistance to antibiotics. *Mol. Microbiol.* **1995**, *16*, 385−295.
(7) Ambler, R. P. The structure of β-lactamases. *Philos. Trans. R. Soc. London* **1980**, *B289*, 321−331.
(8) Bush, K.; Jacoby, G. A.; Medeiros, A. A. A functional classification scheme for β-lactamases and its correlation with molecular structure. *Antimicrob. Agents Chemother.* **1995**, *39*, 1211−1233.
(9) Bush, K. Metallo-β-lactamases: a class apart. *Clin. Infect. Dis.* **1998**, *27*, S48−S53.
(10) Livermore, D. M.; Woodford, N. Carbapenem-hydrolyzing β-lactamases. *Curr. Opin. Microbiol.* **2000**, *3*, 489−495.
(11) Rasmussen, B. A.; Bush, K. Carbapenem-hydrolyzing β-lactamases. *Antimicrob. Agents Chemother.* **1997**, *41*, 223−232.
(12) Galleni, M.; Lamotte-Brasseur, J.; Rossolini, G. M.; Spencer, J.; Dideberg, O.; Frere, J.-M. Standard numbering scheme for class B β-lactamases. *Antimicrob. Agents Chemother.* **2001**, *45*, 660−663.
(13) Wang, Z.; Fast, W.; Valentine, A. M.; Benkovic, S. J. Metallo-β-lactamase: structure and mechanism. *Curr. Opin. Chem. Biol.* **1999**, *3*, 614−622.
(14) Carfi, A.; Pares, S.; Duee, E.; Galleni, M.; Duez, C.; Frere, J.-M.; Dideberg, O. The 3-D structure of a zinc metallo-β-lactamase from *Bacillus cereus* reveals a new type of protein fold. *EMBO J.* **1995**, *14*, 4914−4921.
(15) Concha, N. O.; Rasmussen, B. A.; Bush, K.; Herzberg, O. Crystal structure of the wide-spectrum binuclear zinc β-lactamase from Bacteroides fragilis. *Structure* **1996**, *4*, 823−836.
(16) Carfi, A.; Duee, E.; Paul-Soto, R.; Galleni, M.; Frere, J.-M.; Dideberg, O. X-ray structure of the ZnII β-lactamase from Bacteroides fragilis in an orthorhombic crystal form. *Acta Crystallogr.* **1998**, *D54*, 47−57.
(17) Carfi, A.; Duee, E.; Galleni, M.; Frere, J.-M.; Dideberg, O. 1.85 A resolution structure of the zincII β-lactamase from *Bacillus cereus*. *Acta Crystallogr.* **1998**, *D54*, 313−323.
(18) Fabiane, S. M.; Sohi, M. K.; Wan, T.; Payne, D. J.; Bateson, J. H.; Mitchell, T.; Sutton, B. J. Crystal structure of the zinc-dependent β-lactamase from *Bacillus cereus* at 1.9 A resolution: Binuclear active site with features of a mononuclear enzyme. *Biochemistry* **1998**, *37*, 12404−12411.
(19) Ullah, J. H.; Walsh, T. R.; Taylor, I. A.; Emery, D. C.; Verma, C. S.; Gamblin, S. J.; Spencer, J. The crystal structure of the L1 metallo-β-lactamase from Stenotrophomonas maltophilia at 1.7 A resolution. *J. Mol. Biol.* **1998**, *284*, 125−136.
(20) Garau, G.; Bebrone, C.; Anne, C.; Galleni, M.; Frere, J.-M.; Dideberg, O. A metallo-β-lactamase enzyme in action: Crystal structures of the monozinc carbapenemase CphA and its complex with biapenem. *J. Mol. Biol.* **2005**, *345*, 785−795.
(21) Orellano, E. G.; Girardini, J. E.; Cricco, J. A.; Ceccarelli, E. A.; Vila, A. J. Spectroscopic characterization of a binuclear metal site in *Bacillus cereus* β-lactamase II. *Biochemistry* **1998**, *37*, 10173−10180.
(22) de Seny, D.; Heinz, U.; Wommer, S.; Kiefer, J. H.; Meyer-Klaucke, W.; Galleni, M.; Frere, J.-M.; Bauer, R.; Adolph, H.-W. Metal ion binding and coordination geometry for wild type and mutants of metallo-β-lactamase from *Bacillus cereus* 569/H/9 (BcII). *J. Biol. Chem.* **2001**, *276*, 45065−45078.
(23) Bicknell, R.; Waley, S. G. Cryoenzymology of *Bacillus cereus* β-lactamase II. *Biochemistry* **1985**, *24*, 6876.
(24) Crowder, M. W.; Wang, Z.; Franklin, S. L.; Zovinka, E. P.; Benkovic, S. J. Characterization of the metal-binding sites of the β-lactamase from Bacteroides fragilis. *Biochemistry* **1996**, *35*, 12126−12132.
(25) Wang, Z.; Benkovic, S. J. Purification, characterization, and kinetic studies of a soluble Bacteroides fragilis metallo-β-lactamase that provides multiple antibiotic resistance. *J. Biol. Chem.* **1998**, *273*, 22402−22408.
(26) Paul-Soto, R.; Bauer, R.; Frere, J.-M.; Galleni, M.; Meyer-Klaucke, W.; Nolting, H. F.; Rossolini, G. M.; de Seny, D.; Hernandez-Valladares, M.; Zeppenzauer, M.; Adolph, H. W. Mono- and binuclear Zn^{2+}-β-lactamase: role of the conserved cysteine in the catalytic mechanism. *J. Biol. Chem.* **1999**, *274*, 13242−13249.
(27) Rasia, R. M.; Vila, A. J. Exploring the role and the binding affinity of a second zinc equivalent in B. cereus metallo-β-lactamase. *Biochemistry* **2002**, *41*, 1853−1860.
(28) Wommer, S.; Rival, S.; Heinz, U.; Galleni, M.; Frere, J.-M.; Franceschini, N.; Amicosante, G.; Rasmussen, B. A.; Bauer, R.; Adolph, H. W. Substrate-activated zinc binding of metallo-β-lactamases. *J. Biol. Chem.* **2002**, *277*, 24142−24147.
(29) Walsh, T. R.; Gamblin, S. J.; Emery, D. C.; MacGowan, A. P.; Bennett, B. Enzyme kinetics and biochemical analysis of ImiS, the metallo-β-lactamase from *Aeromonas* sobria 163a. *J. Antimicrob. Chemother.* **1996**, *37*, 423−431.
(30) Valladares, H. M.; Felici, A.; Weber, G.; Adolph, H. W.; Zeppezauer, M.; Rossolini, G. M.; Amicosante, G.; Frere, J.-M.; Galleni, M. Zn(II) dependence of the *Aeromonas* hydrophila AE036 metallo-β-lactamase activity and stability. *Biochemistry* **1997**, *36*, 11534−11541.
(31) Toney, J. H.; Fitzgerald, P. M.; Grover-Sharma, N.; Olsen, S. H.; May, W. J.; Sundelof, J. G.; Vanderwall, D. E.; Clearry, K. A.; Grant, S. K.; Wu, J. K.; Kozarich, J. W.; Pompliano, D. L.; Hammond, G. G. Antibiotic sensitization using biphenyl tetrazoles as potent inhibitors of Bacteroides fragilis metallo-β-lactamase. *Chem. Biol.* **1998**, *5*, 185−196.
(32) Concha, N. O.; Janson, C. A.; Rowling, P.; Pearson, S.; Cheever, C. A.; Clarke, B. P.; Lewis, C.; Galleni, M.; Frere, J.-M.; Payne, D. J.; Bateson, J. H.; Abdel-Meguid, S. S. Crystal structure of the IMP-1 metallo β-lactamase from *Pseudomonas aeruginosa* and its complex with a mercaptocarboxylate inhibitor: Binding determinants of a potent, broad-spectrum inhibitor. *Biochemistry* **2000**, *39*, 4288−4298.
(33) Garcia-Saez, I.; Mercuri, P. S.; Papamicael, C.; Kahn, R.; Frere, J.-M.; Galleni, M.; Rossolini, G. M.; Dideberg, O. Three-dimensional structure of FEZ-1, a monomeric subclass B3 metallo-β-lactamase from Fluoribacter gormanii, in native form and in complex with D-captopril. *J. Mol. Biol.* **2003**, *325*, 651−660.
(34) Garcia-Saez, I.; Hopkins, J.; Papamicael, C.; Franceschini, N.; Amicosante, G.; Rossolini, G. M.; Galleni, M.; Frere, J.-M.; Dideberg, O. The 1.5-A structure of Chryseobaterium meningosepticum zinc β-lactamase in complex with the inhibitor D-captopril. *J. Biol. Chem.* **2003**, *278*, 23868−23873.
(35) Diaz, N.; Suarez, D.; Merz, K. M., Jr. Molecular dynamics simulations of the mononuclear zinc-β-lactamase from *Bacillus cereus* complexed with benzylpenicillin and a quantum chemical study of the reaction mechanism. *J. Am. Chem. Soc.* **2001**, *123*, 9867−9879.
(36) Salsbury, J. F. R.; Crowley, M. F.; Brooks, C. L., III. Modeling of the metallo-β-lactamase from B.fragilis: Structural and dynamic effects of inhibitor binding. *Proteins* **2001**, *44*, 448−459.
(37) Suarez, D.; Diaz, N.; Merz, K. M., Jr. Molecular dynamics simulations of the dinuclear zinc-β-lactamase from Bacteroides fragilis complexed with imipenem. *J. Comput. Chem.* **2002**, *23*, 1587−1600.

(38) Antony, J.; Gresh, N.; Olsen, L.; Hemmingsen, L.; Schofield, C. J.; Bauer, R. Binding of D- and L-captopril inhibitors to metallo-β-lactamase studied by polarizable molecular mechanics and quantum mechanics. *J. Comput. Chem.* **2002**, *23*, 1281−1296.
(39) Krauss, M.; Gresh, N.; Antony, J. Binding and hydrolysis of ampicillin in the active site of a zinc lactamase. *J. Phys. Chem. B* **2003**, *107*, 1215−1229.
(40) Oelschlaeger, P.; Schmid, R. D.; Pleiss, J. Modeling domino effects in enzymes: Molecular basis of the substrate specificity of the bacterial metallo-β-lactamase IMP-1 and IMP-6. *Biochemistry* **2003**, *42*, 8945−8956.
(41) Olsen, L.; Rasmussen, T.; Hemmingsen, L.; Ryde, U. Binding of benzylpenicillin to metallo-β-lactamase: A QM/MM study. *J. Phys. Chem. B* **2004**, *108*, 17639−17648.
(42) Peraro, M. D.; Vila, A. J.; Carloni, P. Substrate binding to mononuclear metallo-β-lactamase from *Bacillus cereus*. *Proteins* **2004**, *54*, 412−423.
(43) Park, H.; Merz, K. M., Jr. Force field design and molecular dynamics simulations of the carbapenem and cephamycin-resistant dinuclear zinc metallo-β-lactamase from Bacteroides fragilis and its complex with a biphenyl tetrazole inhibitor. *J. Med. Chem.* **2005**, *48*, 1630−1637.
(44) Park, H.; Brothers, E. N.; Merz, K. M., Jr. Hybrid QM/MM and DFT investigations of the catalytic mechanism and inhibition of the dinuclear zinc metallo-β-lactamase CcrA from Bacteroides fragilis. *J. Am. Chem. Soc.* **2005**, *127*, 4232−4241.
(45) Scrofani, S. D. B.; Chung, J.; Huntley, J. J. A.; Benkovic, S. J.; Wright, P. E.; Dyson, H. J. NMR characterization of the metallo-β-lactamase from Bacteroides fragilis and its interaction with a tight-binding inhibitor: Role of an active-site loop. *Biochemistry* **1999**, *38*, 14507−14514.
(46) Huntley, J. J. A.; Scrofani, S. D. B.; Osborne, M. J.; Wright, P. E.; Dyson, H. J. Dynamics of the metallo-β-lactamase from bacteriodes fragilis in the presence and absence of a tight-binding inhibitor. *Biochemistry* **2000**, *39*, 13356−13364.
(47) Warshel, A.; Levitt, M. Theoretical studies of enzymatic reactions: Dielectric, electrostatic and steric stabilization of carbonium ion in the reaction of lysozyme. *J. Mol. Biol.* **1976**, *103*, 227−249.
(48) Singh, U. C.; Kollman, P. A. A combined ab initio quantum mechanical and molecular mechanical method for carrying out simulations on complex molecular systems: Applications to the $CH_3Cl + Cl^-$ exchange reaction and gas-phase protonation of polyethers. *J. Comput. Chem.* **1986**, *7*, 718−730.
(49) Field, M. J.; Bash, P. A.; Karplus, M. A combined quantum mechanical and molecular mechanical potential for molecular dynamics simulations. *J. Comput. Chem.* **1990**, *11*, 700−733.
(50) Gao, J.; Amara, P.; Alhambra, C.; Field, M. J. A generalized hybrid orbital (GHO) method for the treatment of boundary atoms in combined QM/MM calculations. *J. Phys. Chem.* **1998**, *A102*, 4714−4721.
(51) Gao, J. Hybrid quantum and molecular mechanical simulations: An alternative avenue to solvent effects in organic chemistry. *Acc. Chem. Res.* **1996**, *29*, 298−305.
(52) Monard, G.; Merz, K. M., Jr. Combined quantum mechanical/molecular mechanical methodologies applied to biomolecular systems. *Acc. Chem. Res.* **1999**, *32*, 904−911.
(53) Garcia-Viloca, M.; Gao, J.; Karplus, M.; Truhlar, D. G. How enzyme work: Analysis by modern rate theory and computer simulations. *Science* **2004**, *303*, 186−195.
(54) Warshel, A. Computer simulations of enzyme catalysis: methods, progress, and insights. *Annu. Rev. Biophys. Biomol. Struct.* **2003**, *32*, 425−443.
(55) Suarez, D.; Merz, K. M., Jr. Molecular dynamics simulations of the mononuclear zinc-β-lactamase from *Bacillus cereus*. *J. Am. Chem. Soc.* **2001**, *123*, 3759−3770.
(56) Peraro, M. D.; Llarrull, L. I.; Rothlisberger, U.; Vila, A. J.; Carloni, P. Water-assisted reaction mechanism of monozinc β-lactamase. *J. Am. Chem. Soc.* **2004**, *126*, 12661−12668.
(57) Brothers, E. N.; Suarez, D.; Deerfield, D. W.; Merz, K. M., Jr. PM3-compatible zinc parameters optimized for metalloenzyme active site. *J. Comput. Chem.* **2004**, *25*, 1677−1692.
(58) Elstner, M.; Porezag, D.; Jungnickel, G.; Elsner, J.; Haugk, M.; Frauenheim, T.; Suhai, S.; Seigert, G. Self-consistent-charge density-functional tight-binding method for simulations of complex materials properties. *Phys. Rev.* **1998**, *B58*, 7260−7268.
(59) Cui, Q.; Elstner, M.; Kaxiras, E.; Frauenheim, T.; Karplus, M. A QM/MM implementation of the self-consistent charge density functional tight binding (SCC-DFTB) method. *J. Phys. Chem. B* **2001**, *105*, 569−585.
(60) Pu, J.; Gao, J.; Truhlar, D. G. Combining self-consistent-charge density-funtional tight-binding (SCC-DFTB) with molecular mechanics by the generalized hybrid orbital (GHO) method. *J. Phys. Chem.* **2004**, *A108*, 5454−5463.
(61) Witek, H. A.; Irle, S.; Morokuma, K. Analytical second-order geometric derivatives of energy for the self-consistent-charge density-functional tight-biding method. *J. Chem. Phys.* **2004**, *121*, 5163−5170.
(62) Witek, H. A.; Morokuma, K. Systematic study of vibrational frequencies calculated with the self-consistent charge density functional tight-binding method. *J. Comput. Chem.* **2004**, *25*, 1858−1864.
(63) Elstner, M.; Hobza, P.; Frauenheim, T.; Suhai, S. Hydrogen bonding and stacking interactions of nucleic acid base pairs: A density-functional-theory based treatment. *J. Chem. Phys.* **2001**, *114*, 5149−5155.
(64) Elstner, M.; Jalkanen, K. J.; Knapp-Mohammady, M.; Frauenheim, T.; Suhai, S. DFT studies on helix formation in *N*-acetyl-(L-alanyl)(*n*)-*N*′-methylamide for n=1−20. *Chem. Phys.* **2000**, *256*, 15−27.
(65) Elstner, M.; Frauenheim, T.; Kaxiras, E.; Seifert, G.; Suhai, S. A self-consistent charge density-functional based tight-binding scheme for large biomolecules. *Phys. Status Solidi* **2000**, *B217*, 357−376.
(66) Elstner, M.; Jalkanen, K. J.; Knapp-Mohammady, M.; Frauenheim, T.; Suhai, S. Energetics and structure of glycine and alanine based model peptides: Approximate SCC-DFTB, AM1 and PM3 methods in comparison with DFT, HF and MP2 calculations. *Chem. Phys.* **2001**, *263*, 203-219.
(67) Guo, H.; Cui, Q.; Lipscomb, W. N.; Karplus, M. Substrate conformational transitions in the active site of chorismate mutase: Their role in the catalytic mechanism. *Proc. Natl. Acad. Sci. U.S.A.* **2001**, *98*, 9032−9037.
(68) Cui, Q.; Elstner, M.; Karplus, M. A theoretical analysis of the proton and hydride transfer in liver alcohol dehydrogenase (LADH). *J. Phys. Chem. B* **2002**, *106*, 2721−2740.
(69) Zhang, X.; Harrison, D. H.; Cui, Q. Functional specificities of methylglyoxal synthase and triosephosphate Isomerase: A combined QM/MM analysis. *J. Am. Chem. Soc.* **2002**, *124*, 14871−14878.
(70) Li, G.; Cui, Q. What is so special about Arg 55 in the catalysis of cyclophilin A? Insights from hybrid QM/MM simulations. *J. Am. Chem. Soc.* **2003**, *125*, 15028−15038.
(71) Elstner, M.; Cui, Q.; Munih, P.; Kaxiras, E.; Frauenheim, T.; Karplus, M. Modeling zinc in biomolecules with the self-consistent charge density functional tight binding (SCC-DFTB) method: Applications to structure and energetic analysis. *J. Comput. Chem.* **2003**, *24*, 565−581.
(72) Xu, D.; Riccardi, D.; Ghosh, N.; Guo, H.; Cui, Q. QM/MM simulations of proton transfer in carbonic anhydrase. *J. Am. Chem. Soc.*, submitted for publication.
(73) Xu, Q.; Guo, H. Quantum mechanical/molecular mechanical molecular dynamics simulations of cytidine deaminase: From stabilization of transition state analogues to catalytic mechanisms. *J. Phys. Chem.* **2004**, *B108*, 2477−2483.
(74) Guo, H.; Rao, N.; Xu, Q.; Guo, H. Origin of tight binding of a near-perfect transition-state analogue by cytidine deaminase: Implications for enzyme catalysis. *J. Am. Chem. Soc.* **2005**, *127*, 3191−3197.
(75) Heinz, U.; Bauer, R.; Wommer, S.; Meyer-Klaucke, W.; Papamicael, C.; Bateson, J.; Adolph, H.-W. Coordination geometries of metal ions in D- or L-captopril-inhibited metallo-β-lactamases. *J. Biol. Chem.* **2003**, *278*, 20659−20666.
(76) Crawford, P. A.; Yang, K.-W.; Sharma, N.; Bennett, B.; Crowder, M. W. Spectroscopic studies on cobalt(II)-substitued metallo-β-lactamase ImiS from *Aeromonas* veronii bv. sobria. *Biochemistry* **2005**, *44*, 5168−5176.
(77) Paul-Soto, R.; Zeppenzauer, M.; Adolph, H. W.; Galleni, M.; Frere, J.-M.; Carfi, A.; Dideberg, O.; Wouters, J.; Hemmingsen, L.; Bauer, R. Preference of Cd(II) and Zn(II) for the two metal sites in *Bacillus cereus* β-lactamase II: A perturbed angular correlation of γ-rays spectroscopic study. *Biochemistry* **1999**, *38*, 16500−16506.
(78) Kumagai, T.; Tamai, S.; Abe, T.; Matsunaga, H.; Hayashi, K.; Kishi, I.; Shiro, M.; Nagao, Y. New straightforward synthesis and characterization of a unique 1β-methylcarbapenem antibiotic biapenem bearing a σ-symmetric bicyclotriazoliumthio group as the pendant moiety. *J. Org. Chem.* **1998**, *63*, 8145−8149.
(79) Brooks, B. R.; Bruccoleri, R. E.; Olafson, B. D.; States, D. J.; Swaminathan, S.; Karplus, M. Charmm: A program for macromolecular energy, minimization, and dynamics calculations. *J. Comput. Chem.* **1983**, *4*, 187−217.
(80) MacKerell, A. D., Jr.; Bashford, D.; Bellott, M.; Dunbrack, R. L., Jr.; Evanseck, J. D.; Field, M. J.; Fischer, S.; Gao, J.; Guo, H.; Ha, S.; Joseph-McCarthy, D.; Kuchnir, L.; Kuczera, K.; Lau, F. T. K.; Mattos, C.; Michnick, S.; Ngo, T.; Nguyen, D. T.; Prodhom, B.; Reiher, W. E., III; Roux, B.; Schlenkrich, M.; Smith, J. C.; Stote, R.; Straub, J.; Watanabe, M.; Wiorkiewicz-Kuczera, J.; Yin, D.; Karplus, M. All-atom empirical potential for molecular modeling and dynamics studies of proteins. *J. Phys. Chem.* **1998**, *B102*, 3586−3616.

(81) Jorgensen, W. L.; Chandrasekhar, J.; Madura, J. D.; Impey, R. W.; Klein, M. L. Comparison of simple potential functions for simulating liquid water. *J. Chem. Phys.* **1983**, *79*, 926−935.
(82) Brooks, C. L., III; Karplus, M. Solvent effects on protein motion and protein effects on solvent motion. *J. Mol. Biol.* **1989**, *208*, 159−181.
(83) Ryckaert, J. P.; Ciccotti, G.; Berendsen, H. J. Numerical integration of the Cartesian equations of motion of a system with constraints: molecular dynamics of *n*-alkanes. *J. Comput. Phys.* **1977**, *23*, 327−341.
(84) Becke, A. D. Density-functional thermochemistry. 3. The role of exact exchange. *J. Chem. Phys.* **1993**, *98*, 5648−5652.
(85) Lee, C.; Yang, W.; Parr, R. G. Development of the Colle-Salvetti correlation-energy formula into a functional of the electron density. *Phys. Rev. B* **1988**, *37*, 785−789.
(86) Frisch, M. J.; Trucks, G. W.; Schlegel, H. B.; Scuseria, G. E.; Robb, M. A.; Cheeseman, J. R.; Montgomery, J. A., Jr.; T. V.; Kudin, K. N.; Burant, J. C.; Millam, J. M.; Iyengar, S. S.; Tomasi, J.; Barone, V.; Mennucci, B.; Cossi, M.; Scalmani, G.; Rega, N.; Petersson, G. A.; Nakatsuji, H.; Hada, M.; Ehara, M.; Toyota, K.; Fukuda, R.; Hasegawa, J.; Ishida, M.; Nakajima, T.; Honda, Y.; Kitao, O.; Nakai, H.; Klene, M.; Li, X.; Knox, J. E.; Hratchian, H. P.; Cross, J. B.; Adamo, C.; Jaramillo, J.; Gomperts, R.; Stratmann, R. E.; Yazyev, O.; Austin, A. J.; Cammi, R.; Pomelli, C.; Ochterski, J. W.; Ayala, P. Y.; Morokuma, K.; Voth, G. A.; Salvador, P.; Dannenberg, J. J.; Zakrzewski, V. G.; Dapprich, S.; Daniels, A. D.; Strain, M. C.; Farkas, O.; Malick, D. K.; Rabuck, A. D.; Raghavachari, K.; Foresman, J. B.; Ortiz, J. V.; Cui, Q.; Baboul, A. G.; Clifford, S.; Cioslowski, J.; Stefanov, B. B.; Liu, G.; Liashenko, A.; Piskorz, P.; Komaromi, I.; Martin, R. L.; Fox, D. J.; Keith, T.; Al-Laham, M. A.; Peng, C. Y.; Nanayakkara, A.; Challacombe, M.; Gill, P. M. W.; Johnson, B.; Chen, W.; Wong, M. W.; Gonzalez, C.; Pople, J. A. *Gaussian 03*, revision A.1; Gaussian, Inc.: Pittsburgh, PA.
(87) Bruice, T. C.; Lightstone, F. C. Ground state and transition state contributions to the rates of intramolecular and enzymatic reactions. *Acc. Chem. Res.* **1999**, *32*, 127−136.
(88) Singh, U. C.; Kollman, P. A. An approach to computing electrostatic charges for molecules. *J. Comput. Chem.* **1984**, *5*, 129−145.
(89) Besler, B. H.; Merz, K. M., Jr.; Kollman, P. A. Atomic charges derived from semiempirical methods. *J. Comput. Chem.* **1990**, *11*, 431−439.
(90) Prosperi-Meys, C.; Wouters, J.; Galleni, M.; Lamotte-Brasseur, J. Substrate binding and catalytic mechanism of class B β-lactamases: A molecular modelling study. *Cell. Mol. Life Sci.* **2001**, *58*, 2136−2143.
(91) Wang, Z.; Fast, W.; Benkovic, S. J. Direct observation of an enzyme-bound intermediate in the catalytic cycle of the metallo-β-lactamase from Bacteroides fragilis. *J. Am. Chem. Soc.* **1998**, *120*, 10788−10789.
(92) Wang, Z.; Fast, W.; Benkovic, S. J. On the mechanism of the metallo-β-lactamse from Bacteroides fragilis. *Biochemistry* **1999**, *38*, 10013−10023.
(93) Fast, W.; Wang, Z.; Benkovic, S. J. Familial mutations and zinc stoichimoetry determine the rate-limiting step of nitrocefin hydrolysis by metallo-β-lactamase from Bacteroides fragilis. *Biochemistry* **2001**, *40*, 1640−1650.
(94) Yanchak, M. P.; Taylor, R. A.; Crowder, M. W. Mutational analysis of metallo-β-lactamase CcrA from Bacteroides fragilis. *Biochemistry* **2000**, *39*, 11330−11139.
(95) Gensmantel, N. P.; Gowling, E. W.; Page, M. I. Metal ion catalysis in the aminolysis of penicillin. *J. Chem. Soc., Perkin Trans. 2* **1978**, 335−342.
(96) Diaz, N.; Suarez, D.; Merz, K. M., Jr. Zinc metallo-β-lactamase from Bacteroides fragilis: A quantum chemical study on model systems of the active site. *J. Am. Chem. Soc.* **2000**, *122*, 4197−4208.
(97) McManus-Munoz, S.; Crowder, M. W. Kinetic mechanism of metallo-β-lactamase L1 from Stenotrophomonas maltophilia. *Biochemistry* **1999**, *38*, 1547−1553.
(98) Spencer, J.; Clarke, A. R.; Walsh, T. R. Novel mechanism of hydrolysis of therapeutic β-lactams by Stenotrophomonas maltophilia L1 metallo-β-lactamase. *J. Biol. Chem.* **2001**, *276*, 33638−33644.
(99) Garrity, J. D.; Bennett, B.; Crowder, M. W. Direct evidence that the reaction intermediate of metallo-β-lactamase L1 Is metal bound. *Biochemistry* **2005**, *44*, 1078−1087.
(100) Bounaga, S.; Laws, A. P.; Galleni, M.; Page, M. I. The mechanism of catalysis and the inhibition of the *Bacillus cereus* zinc-dependent β-lactamase. *Biochem. J.* **1998**, *331*, 703−711.
(101) Rasia, R. M.; Vila, A. J. Structural determinants of substrate binding to *Bacillus cereus* metallo-β-lactamase. *J. Biol. Chem.* **2004**, *279*, 26046−26051.
(102) Lim, H. M.; Iyer, R. K.; Pene, J. J. Site-directed mutagenesis of dicarboxylic acids near the active site of *Bacillus cereus* 5/B/6 β-lactamase II. *Biochem. J.* **1991**, *276*, 401−404.
(103) Suarez, D.; Brothers, E. N.; Merz, K. M., Jr. Insights into the structure and dynamics of the dinuclear zinc β-lactamase site from Bacteroides fragilis. *Biochemistry* **2002**, *41*, 6615−6630.
(104) Peraro, M. D.; Vila, A. J.; Carloni, P. Protonation state of Asp120 in the binuclear active site of the metallo-β-lactamase from Bacteroides fragilis. *Inorg. Chem.* **2003**, *42*, 4245−4247.
(105) Garrity, J. D.; Carenbauer, A. L.; Herron, L. R.; Crowder, M. W. Metal binding Asp-120 in metallo-β-lactamase L1 from Stenotrophomonas maltophilia plays a crucial role in catalysis. *J. Biol. Chem.* **2004**, *279*, 920−927.
(106) Felici, A.; Amicosante, G.; Oratore, A.; Strom, R.; Ledent, P.; Joris, B.; Fanuel, L.; Frere, J.-M. An overview of the kinetic parameters of class B β-lactamases. *Biochem. J.* **1993**, *291*, 151−155.
(107) Jencks, W. P. *Catalysis in Chemistry and Enzymology*; Dover: New York, 1986.
(108) Christianson, D. W. Arginase: structure, mechanism, and physiological role in male and female sexual arousal. *Acc. Chem. Res.* **2005**, *38*, 191−201.
(109) Ivanov, I.; Klein, M. L. Dynamical flexibility and proton transfer in the arginase active site probed by ab initio molecular dynamics. *J. Am. Chem. Soc.* **2005**, *127*, 4010−4020.
(110) Warshel, A. *Computer Modeling of Chemical Reactions in Enzymes and Solutions*; Wiley: New York, 1991.
(111) Gao, J.; Truhlar, D. G. Quantum mechanical methods for enzyme kinetics. *Annu. Rev. Phys. Chem.* **2002**, *53*, 467−505.
(112) Benkovic, S. J.; Hammes-Schiffer, S. A perspective on enzyme catalysis. *Science* **2003**, *301*, 1196−1202.

JM0505112